Applied Catalysis B: Environmental 89 (2009) 411–419

Contents lists available at ScienceDirect

Applied Catalysis B: Environmental

journal homepage: www.elsevier.com/locate/apcatb

Palladium and platinum catalysts supported on carbon nanofiber coated monoliths for low-temperature combustion of BTX

S. Morales-Torres [a], A.F. Pérez-Cadenas [a,*], F. Kapteijn [b], F. Carrasco-Marín [a], F.J. Maldonado-Hódar [a], J.A. Moulijn [b]

[a] Departamento de Química Inorgánica, Facultad de Ciencias, Universidad de Granada, Campus Fuentenueva s/n, 18071 Granada, Spain
[b] Catalysis Engineering, DelftChemTech, Faculty of Applied Sciences, Delft University of Technology, Julianalaan 136, 2628 BL Delft, The Netherlands

ARTICLE INFO

Article history:
Received 26 October 2008
Received in revised form 15 December 2008
Accepted 20 December 2008
Available online 30 December 2008

Keywords:
Carbon nanofibers
Coating
Monolithic catalysts
BTX combustion
Platinum
Palladium

ABSTRACT

In this work carbon nanofiber (CNF)-coated monoliths with a very thin, homogeneous, consistent and good adhered CNF layer were obtained by means of catalytic decomposition of ethylene on Ni particles.

The catalytic behaviour of Pt and Pd supported on the CNF-coated monoliths was studied in the low-temperature catalytic combustion of benzene, toluene and *m*-xylene (BTX) and compared with the performance of Pt and Pd supported on γ-Al_2O_3 coated monoliths.

The catalysts supported on CNF-coated monoliths were the most active, independent of the metal catalyst or the type of the tested aromatic compound. TPD experiments showed that the γ-Al_2O_3 phase retained important amounts of the water molecules produced during the reaction. When water vapour was supplied to the reactant flow, the activity of Pd catalysts decreased much stronger than the Pt ones, and the activity of the Pt catalysts supported on the γ-Al_2O_3 was more affected than that of the catalysts supported on CNF.

BTX combustion reactions seem to be catalyzed by Pt and Pd through different kinetic mechanisms, explaining why Pt catalysts always were more active than the Pd ones deposited on the same type of support. Pd catalyzed combustion of benzene is strongly inhibited by oxygen and by water.

Catalysts supported on CNF-coated monoliths showed a selectivity to burn benzene better than toluene or *m*-xylene, attributed to a better aromatic-CNF surface interaction.

1. Introduction

Catalytic combustion is one of the most important technologies for eliminating VOC present at low concentration in effluent streams. From an energetic point of view, and to avoid NO_x formation, low temperatures (below 200 °C) are preferred. However, at these conditions, water vapour produced during combustion can be retained on the catalytic support [1,2], with negative effects (inhibition) on the activity of the catalyst, as it was reported for benzene combustion over Pt/TiO_2 catalysts [3]. Hydrophobic catalyst supports may alleviate this effect [4], so the tuneable surface hydrophobicity of carbon materials is an important consideration for their application as catalyst support in VOC combustion [2,5–7].

In practice, ceramic monolithic supports have been employed in different environmental catalytic applications [8–12], because of their low-pressure drop, short diffusion distances, the lack of attrition by vibrations and thermal shock resistance [13]. Previous work showed that carbon-coated monoliths are good supports for Pt and Pd catalysts in the catalytic gas phase combustion of xylenes (total selectivity to CO_2 and H_2O, and good activities below 200 °C) [14], where the performance in the Pd catalyzed total combustion of *m*-xylene is strongly affected by the carbon porosity improving the contact between the metal particles and the aromatic molecules [15]. The VOC-support interaction is highly important for the catalytic process. Burgos et al. showed for the total oxidation of VOC mixtures (including toluene) over Pt supported on Al_2O_3/Al monoliths [16] that the adsorption of the VOC on the Al_2O_3 could be correlated with its polarity. Toebes et al. concluded that the hydrogenation of cinnamaldehyde over carbon nanofibers (CNF)-supported Pt catalysts was assisted by adsorption of the benzene ring on the non-polar CNF support surface [17].

Some studies [3,8,16,18–22] report on the kinetics of the BTX combustion over Pt, and mostly related to benzene at concentrations below 1000 ppm. In these cases, the reaction orders with respect to the VOC were always positive with values generally very close to zero [3,21,22]. In contrast, the kinetics of the BTX combustion over Pd has been much less studied [21].

* Corresponding author. Tel.: +34 958243235; fax: +34 958248526.
E-mail address: afperez@ugr.es (A.F. Pérez-Cadenas).

0926-3373/$ – see front matter © 2008 Elsevier B.V. All rights reserved.
doi:10.1016/j.apcatb.2008.12.021

Only a few studies compare the combustion of benzene, toluene and xylene catalyzed by Pt/Al_2O_3 [8,23] and Pt/carbon [2]. The reactivity of these compounds decreases in the order: benzene > toluene > xylenes. For Pd catalysts such a comparison is lacking.

Finally, although the CNF catalytic synthesis and applications have been extensively studied [24], their use as catalyst supports in this kind of combustion reactions has not been reported.

The objective of this work to demonstrate that carbon materials are better catalyst supports than a typical inorganic one (as γ-Al_2O_3) for the gas phase BTX combustion below 200 °C. The catalytic behaviour of Pd and Pt supported on CNF-coated monoliths is studied in the low-temperature catalytic combustion of benzene, toluene and *m*-xylene (BTX), and compared with the corresponding behaviour of Pd and Pt supported on γ-Al_2O_3 coated monoliths. Carbon nanofibers are chosen as catalyst supports because (i) among the carbon materials they have a good resistance to oxidation, (ii) the amount, thickness and homogeneity of the coating on a monolith is well controllable, and (iii) the interwoven nanofibers layer contains only meso- and macropores without micropores, the kind of porosity that works best in these reactions [15].

2. Experimental

2.1. Preparation of the monolithic supports and catalysts

Cordierite monolithic substrates have been coated with a γ-Al_2O_3-layer using a dipcoating method. The cylindrical (length 1.5 cm, diameter 1 cm) cordierite monolithic substrates had square channels, a cell density of 62 cells cm^{-2} (400 cpsi) and a wall thickness of 0.18 mm (Corning Inc.).

The procedure consists of dipping the cordierite monolith into a γ-Al_2O_3/water suspension in acid pH using a modified version [25] of the method proposed by Nijhuis et al. [26]. In this case the alumina/water suspension was prepared in a 3-L alumina ball-mill with agate balls (Gerhards ball-mill D-652354). For this purpose 300 g of γ-alumina (Condea Puralox, SBA-200, average particle size: 40 μm) was milled together with 400 mL of demineralized water and 170 g of Al_2O_3 20 wt.% in colloidal dispersion, Alfa Aesar. Nitric acid was added to lower the pH to 3.5. The slurry was milled for approximately 24 h. After dipping the excess of suspension in the monolithic channels was removed by flushing with a controlled flow of air (air-knife), the monolith is then dried in the horizontal position, being rotated continuously around its axis, to prevent gravity from causing an uneven washcoat distribution. Finally, the monoliths were calcined at 400 °C for 4 h with a heating rate of 2 °C min^{-1} in order to avoid cracks. The coated-monoliths contained around 11 wt.% of γ-Al_2O_3 and they will be referred as A monoliths.

For CNF coating, Ni was deposited by equilibrium impregnation of these monolithic supports with an aqueous solution of nickel(II) nitrate of pH 4.5. After drying these samples were calcined again at 400 °C for 2 h, and the Ni loading was around 0.2 wt.%. After *in situ* reduction for 1 h at 550 °C, CNF were grown on the monoliths under ethylene:N_2 (1:9) atmosphere for 4 h at 550 °C. CNF-coated monoliths were oxidized with an aqueous solution of H_2O_2 9.8 M at room temperature to create anchoring sites for metal deposition [27]. After this treatment the monoliths were washed several times with demineralized water, and finally the water in the monolithic channels was removed by flushing with air. The final content of CNF in the monoliths was 3.3 wt.% ('ACNF monoliths').

The catalysts were deposited on the monoliths A and ACNF by equilibrium impregnation of the supports with an aqueous solution of tetraamine platinum(II) nitrate or tetraamine palladium(II) nitrate, yielding the monolithic catalysts Pt/A, Pt/ACNF and Pd/A, Pd/ACNF, respectively. Both the impregnation methods and the liquid phase oxidation treatment were carried out in a glass set-up especially designed for the treatments of monoliths in a liquid phase, where the liquid was forced by internal recycling through the channels of the monoliths during 24 h [28].

2.2. Characterization of the monolithic supports

The different preparation steps were studied by scanning electron microscopy (SEM) using a Philips XL-20 microscope and gold sputtering of the samples. Carbon nanofiber morphology was studied by high-resolution transmission electron microscopy (HRTEM) using a Phillips CM-20 microscope equipped with an EDAX microanalysis system.

The textural surface properties of the catalyst supports were determined by physical adsorption of N_2 at −196 °C, and by mercury porosimetry. The BET [29] equation was used for analysis of N_2 adsorption isotherms. The molecular area of N_2 at −196 °C was taken as 0.162 nm^2. Mercury porosimetry was performed up to a pressure of 4200 kg cm^{-2} using Quantachrome Autoscan 60 equipment. With this technique, the following parameters were obtained: the pore volume corresponding to pores with diameter between 3.7 and 50 nm, V_{MESO}, referred to as mesopore volume (note that mesopore volume range [30] is classically defined as 2–50 nm); and the pore volume of pores with diameter greater than 50 nm, or macropore volume, V_{MACRO}. The surface chemistry of the carbon nanofiber coated monoliths was characterized by temperature-programmed desorption (TPD). TPD experiments were carried out by heating the samples to 1000 °C in He flow (60 cm^3 min^{-1}). The amount of evolved gases was recorded as a function of temperature using a quadrupole mass spectrometer (Balzers, model Thermocube) [31].

The monolithic supports were analyzed by immersion calorimetry [30]. The immersion enthalpies into water of the outgassed samples (110 °C for 12 h) were measured at 30 °C with an isothermal calorimeter of the Tian-Calvet type, Setaram C-80. Corrections corresponding to the bulb breaking energy and to the liquid vaporization energy have been made.

2.3. Characterization of the monolithic catalysts

The Pt or Pd loadings of the monolithic catalysts, as well as, the Ni loading of the monolithic support before the CNF growth, were analyzed by inductively coupled plasma mass spectrometry (ICP-MS) using a PerkinElmer Sciex Elan-5000 spectrometer.

Pd- and Pt-dispersions, D, and their average particle sizes ($\bar{d}$) were obtained by CO- or H_2-chemisorption at 25 °C, and assuming a CO:Pd = 1:1 and H_2:Pt = 1:2 stoichiometry, respectively. The average particle sizes were calculated as $\bar{d}_{Pd} = 1.12/D\,(nm)$ or $\bar{d}_{Pt} = 1.08/D\,(nm)$ for Pd and Pt, respectively. Gas-chemisorption isotherms were measured in conventional volumetric equipment made of Pyrex glass and free of mercury and grease, which reached a dynamic vacuum better than 10^{-6} mbar at the sample location. Equilibrium pressure was measured with a Baratron transducer from MKS. All catalysts were pre-treated at 300 °C in H_2 flow (purity of 99.999%) for 3 h, both prior to the characterization by gas-chemisorption and for the BTX combustion reactions.

The thermal stability of the monolithic catalysts in the reaction conditions was studied in a thermogravimetric analyzer (TGA, Mettler Toledo, TGA/SDTA851e). Oxidation experiments were carried out by heating the catalysts at 2 °C min^{-1} up to 800 °C in an air flow of 100 cm^3 min^{-1}.

XPS measurements of the pre-treated catalysts were made with an Escalab 200R system (VG Scientific Co.) equipped with Mg Kα X-ray source ($h\nu$ = 1253.6 eV) and hemispherical electron analyzer. For these measurements, the binding energy (BE) values were

referred to the C_{1s} peak at 284.9 eV. Prior to the analysis, the samples were crushed and pre-treated in H_2 at 300 °C. Once the pre-treatment was finished, the sample was cooled to room temperature under He flow, evacuated at high vacuum and then introduced into the analysis chamber. A base pressure of 10^{-9} mbar was maintained during data acquisition. Survey and multi-region spectra were recorded at C_{1s}, O_{1s}, Al_{2p}, Si_{2p}, Ni_{2p}, Pd_{3d} and/or Pt_{4d} photoelectron peaks. It should be noted that the Pt_{4d} region spectra was analyzed instead of the Pt_{4f} region, because the samples showed an Al_{2p} peak so intense that it did not allow to deconvolute the more intense Pt_{4f} signal. Each spectral region of photoelectron interest was scanned several times to obtain good signal-to-noise ratios. The spectra obtained after background signal correction were fitted to Lorentzian and Gaussian curves in order to obtain the number of components, the position of each peak and the peak areas.

2.4. Catalytic combustion of benzene, toluene and m-xylene in gas phase

All the monolithic catalysts and supports were tested in the catalytic combustion of benzene, toluene and *m*-xylene. Experiments were carried out in a glass reactor in the gas phase, operating in continuous mode at atmospheric pressure. In all cases, one piece of monolithic catalyst (length 1.5 cm) was used. The total flow of the reactant mixture with approximately 1000 ppm of VOC (aromatic compound/O_2/He = 0.1/20.0/79.9%) was tuned to a gas hourly space velocity (GHSV) of 2000 $m^3_{gas} h^{-1} m^{-3}_{monolith}$. The reaction was performed at temperatures between 120 and 190 °C, and always from high to low temperature. The influence of water on the catalytic activity in the oxidation of benzene was examined with a feed mixture, containing 22,000 ppm of water vapour.

Prior to the catalytic activity measurements, the monolithic catalysts were pre-treated in H_2 flow as described above. Reaction products were analyzed online by gas chromatography using a PerkinElmer gas chromatograph, model 8500, with a thermal conductivity detector and Paraplot Q capillary column. The only reaction products found were CO_2 and H_2O. Other products were not detected under the experimental conditions used. In all the cases, the same conversion was obtained on the basis of both BTX consumption and CO_2 formation.

3. Results and discussion

3.1. Characterization of the monolithic support

Thin, homogeneous, consistent and good adhered γ-Al_2O_3 and CNF layers were obtained on the monolithic structures. Fig. 1 shows the secondary electron (SE) images of the monolithic supports. Fig. 1a–c shows different views from sample A. In particular, a detail of the γ-Al_2O_3-layer can be observed in (Fig. 1c). The average thickness of this layer was estimated around 8 μm. The washcoat was homogeneously distributed over the whole channel surface (Fig. 1a). Although there are alumina particles inside the cordierite walls (Fig. 1b), only some isolated CNF have been observed in these places. Views of the surface texture before and after the CNF coating are shown in Fig. 1c and d, respectively. Due to the extremely thin CNF-layer formed on the γ-Al_2O_3 one, the original γ-Al_2O_3 macropores still can be observed.

The diameters of the CNF vary, nanofibers up to 200 nm diameter have been observed. Nevertheless, the majority of nanofibers observed by HRTEM showed diameters around 20 nm (Fig. 2). Ni particles were observed embedded in the extremes (confirmed by EDAX).

The chemical composition of the monolithic supports is collected in Table 1. In order to evaluate properly the textural differences between both catalysts support, it is important to note the low amount of CNF in the coating. The apparent surface area (S_{BET}) significantly increased with the CNF coating (Table 2), taken into account that S_{BET} values are given per gram of total coatings, that is, per gram of γ-Al_2O_3 in sample A, and per gram of γ-Al_2O_3 + CNF in the case of sample ACNF. The V_{MACRO} and V_{MESO} values (expressed per total sample mass) show that both samples

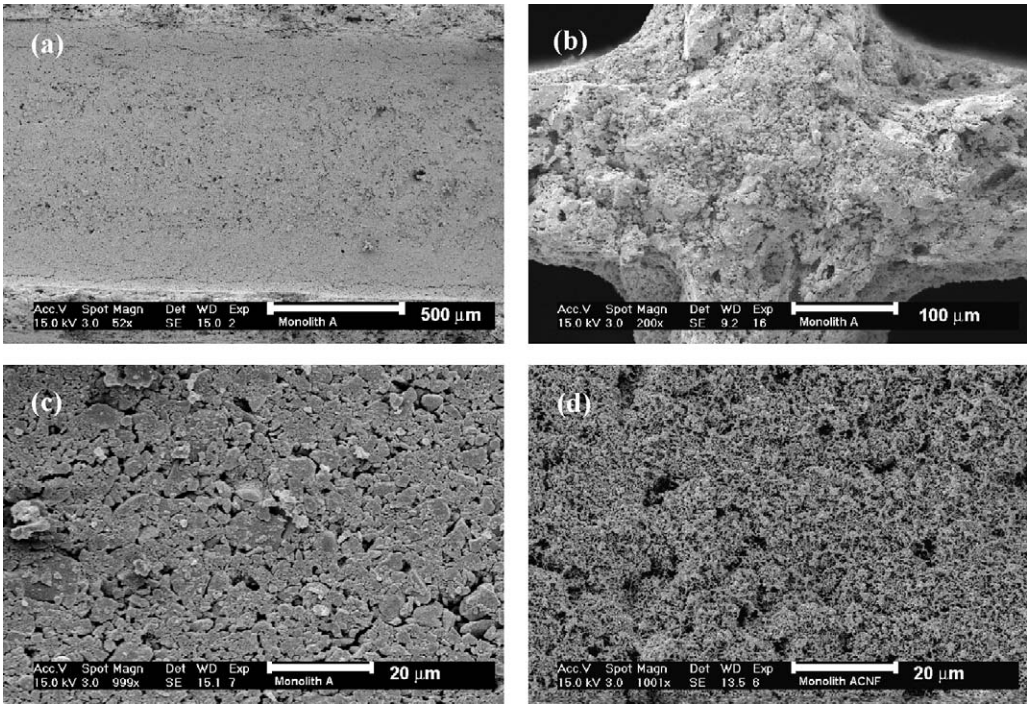

Fig. 1. Secondary electron images of the monoliths: (a) and (b) are top and cross-sectional views, respectively, of the sample A. (c) and (d) are details with the same magnification from top sectional views of the γ-Al_2O_3-layer in sample A, and of the CNF coating in sample ACNF, respectively.

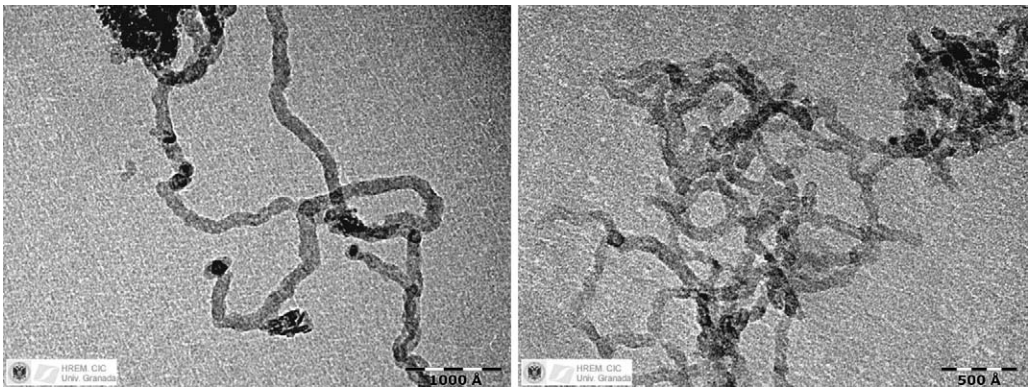

Fig. 2. HRTEM images of the carbon nanofibres from sample ACNF.

Table 1
Composition of the monolithic supports.

Monolithic support	Cordierite (% wt.)	γ-Al_2O_3 (% wt.)	CNF (% wt.)
A	89.0	11.0	0.0
ACNF	86.1	10.6	3.3

Table 2
Characteristics of the monolithic supports.

Monolithic support	S_{BET} ($m^2\ g^{-1}$)*	[a]V_{MACRO} ($cm^3\ g^{-1}$)	[a]V_{MESO} ($cm^3\ g^{-1}$)	[b]Enthalpy ($J\ g^{-1}$)*
A	164	0.134	0.027	−138.2
ACNF	371	0.157	0.028	−103.8

[a] By mercury porosimetry.
[b] By immersion calorimetry in water.
* Data given per gram of total coating material.

are mainly macroporous (Table 2). The macropore volume was larger in monolith ACNF than in A and the macropores were narrower after the CNF coating (Fig. 3). From mercury porosimetry the mesoporosity of both samples seems to be similar.

With regard to the chemical surface characterization the data of sample ACNF obtained by TPD after its oxidation treatment are collected in Table 3, that is, just before Pt or Pd deposition. It is observed that a large amount of oxygen surface complexes was fixed, mainly the type decomposing into CO.

Both samples were also studied by immersion calorimetry in order to quantify their *a priori* different water-support interactions. The ACNF immersion enthalpy was lower than for sample A (Table 2). So, the presence of CNF in the sample influences significantly the water immersion, resulting in a more hydrophobic ACNF sample.

Finally, Ni was not detected by XPS in sample ACNF probably because the Ni loading is below the detection limit, although HRTEM revealed the presence of Ni particles at the ends of the majority of the fibers.

3.2. Characterization of the monolithic catalysts

Pt or Pd loadings, dispersion and particle size of the catalysts are presented in Table 4. Catalysts with the same support have similar metal loadings based on the total sample mass. However the ACNF catalysts had a lower metal loading than the ones supported on A, even though ACNF had a larger apparent surface area. Taking in account the catalyst preparation method, these results correlate with and are attributed to the water immersion properties of the catalyst supports; that is, the wetting interaction of the monolithic support A with the aqueous solution of the catalyst precursor is better. Obviously, in monoliths ACNF Pt or Pd particles will be deposited on both phases: γ-Al_2O_3 and CNF.

The platinum catalysts have very similar dispersion, so catalytic results are not influenced by a structure sensitivity effect, where below a critical Pt particle size the BTX combustion activity decreases with decreasing Pt particle size [6,14,20,21]. The lower Pd-dispersion, compared to the Pt monolithic catalysts has been observed before [14], and it might be related with a lower thermal stability of the Pd complex, which would favour the sintering of this metal before reduction [32], although the Pd-dispersion could also have been influenced by the method used to determine it [33]. No hydrogen or carbon monoxide chemisorption was observed for the monolithic supports.

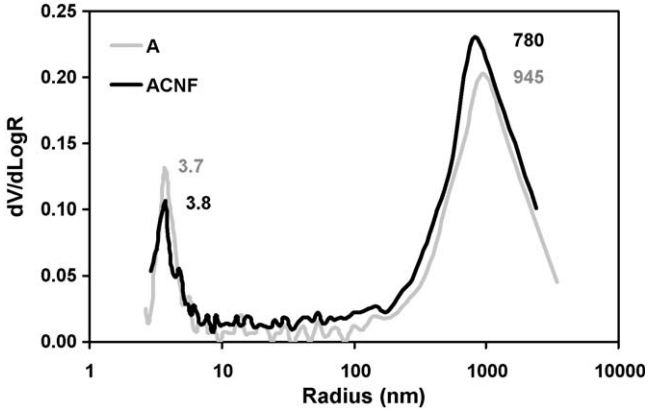

Fig. 3. Pore size distribution of the monolithic support from mercury porosimetry.

Table 3
Amounts of CO and CO_2 evolved up to 1000 °C and back-calculated oxygen content of the monolith ACNF determined by TPD. Data are given per gram of carbon.

Monolith	CO_2 ($\mu mol\ g_{carbon}^{-1}$)	CO ($\mu mol\ g_{carbon}^{-1}$)	O (% $wt._{carbon}$)
ACNF	909	4242	10.3

Table 4
Loading, dispersion (D) and Pt or Pd particle size ($\bar{d}$) of the monolithic catalysts.

Monolithic catalyst	Metal (ICP) (% wt.)	Metal (XPS) (% wt.)	D (%)	$\bar{d}$ (nm)
Pt/A	0.90	1.0	26.2	4.1
Pt/ACNF	0.38	b.d.	24.3	4.4
Pd/A	0.82	1.2	4.6	24.2
Pd/ACNF	0.45	0.6	10.3	10.9

b.d. below detection limit.

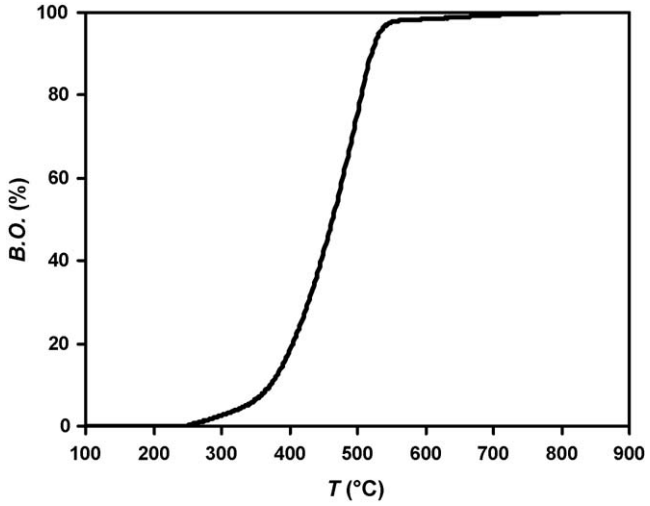

Fig. 4. Burn-off profile in air as a function of temperature for the monolithic catalyst Pt/ACNF.

Table 4 also shows the metal loadings obtained by XPS. As we have crushed the samples for XPS analysis this indicates that in the sample Pt/A platinum is distributed homogeneously throughout the sample whereas for the samples Pd/A and Pd/ACNF significant palladium surface enrichment must have taken place. The Pt XPS-signals were negligible in sample Pt/ACNF is ascribed to the low Pt loading and the less intense Pt_{4d} region spectra studied [34]. After the treatment with H_2, that is just before the combustion experiments, only Pt^0 ($Pt4d_{5/2}$ BE 315.0 eV) or Pd^0 ($Pd3d_{5/2}$ BE 335.0 eV) were observed in the monolithic catalysts.

A potential inconvenience of using carbon materials as catalyst support in combustion reactions is their susceptibility towards consumption as well. For this reason, the oxidation resistance of the monolithic catalysts supported on ACNF was studied by TGA. Results obtained with catalysts Pt/ACNF are depicted in Fig. 4 and show that the burn-off of the material started around 250 °C. This temperature is much higher than that used to study the catalytic oxidation of BTX. In order to avoid any risk in a practical application, additional experiments at 190 °C under a 3.6 L h^{-1} air flow for 12 h were carried out, and no weight loss of the monolithic support was observed. Therefore, significant oxidation of the support is not expected to take place during the study of the BTX combustion. Thermal stability of the supported catalysts was also checked at reaction conditions (120–190 °C). For this purpose, the aromatic compound/O_2/He flow was switched to an air flow and no CO_2 was detected in the gas leaving the reactor confirming the stability of the support material and the absence of strongly adsorbed material that may have accumulated on the catalyst surface.

3.3. Catalytic combustion of benzene, toluene and m-xylene in gas phase

The behaviour of the monolithic catalysts was evaluated by measuring the conversion versus reaction temperature, as well as versus time on stream. Moreover, some catalytic experiments of conversion in function of the space velocity were carried out as well.

All catalysts were active in this reaction being CO_2 and H_2O the only products detected. In all experiments no variation of CO_2 conversion as a function of time on stream was observed for 10 h. The supports monolith A and ACNF did not show any catalytic activity. Apparently Ni used for the CNF growth did not improve the catalytic performance in the range of temperatures studied.

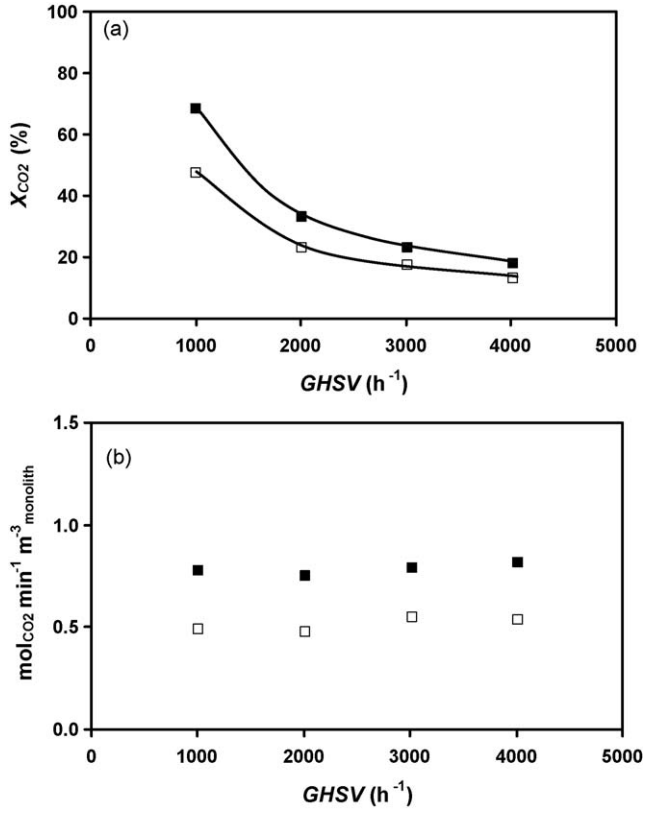

Fig. 5. Conversion to CO_2 (a) and production rate of CO_2 (b) as function of the gas hourly space velocity (GHSV) for sample Pt/ACNF. Key: Closed symbols toluene combustion at 170 °C; open symbols benzene combustion at 150 °C.

This is attributed to the fact that Ni particles seem to be embedded inside the nanofibers, and that Ni catalysts probably require much higher temperatures to be active in this kind of combustion reactions.

Kinetic aspects were investigated by varying the space velocity over catalyst Pt/ACNF for the combustion of benzene and toluene. Fig. 5a shows that conversion to CO_2 decreases as the space velocity increases, following a hyperbolic trend due to a decreasing space time. However the total CO_2 formation per time unit does not change (Fig. 5b) which suggests the absence of external diffusion problems or a poor distribution of the flows through the monolithic channels [35].

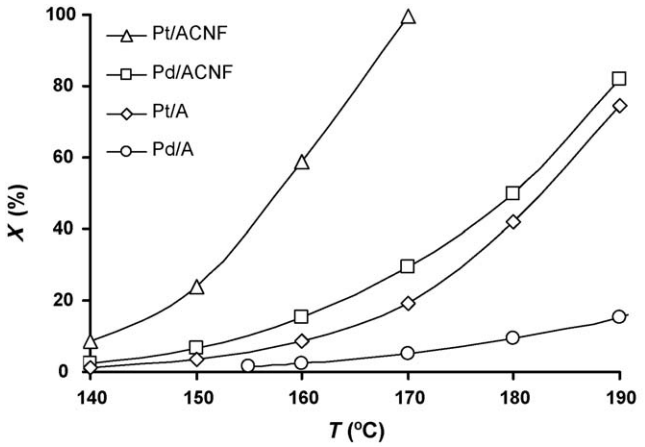

Fig. 6. Light-off curves for benzene combustion over all catalysts: conversion as a function of temperature.

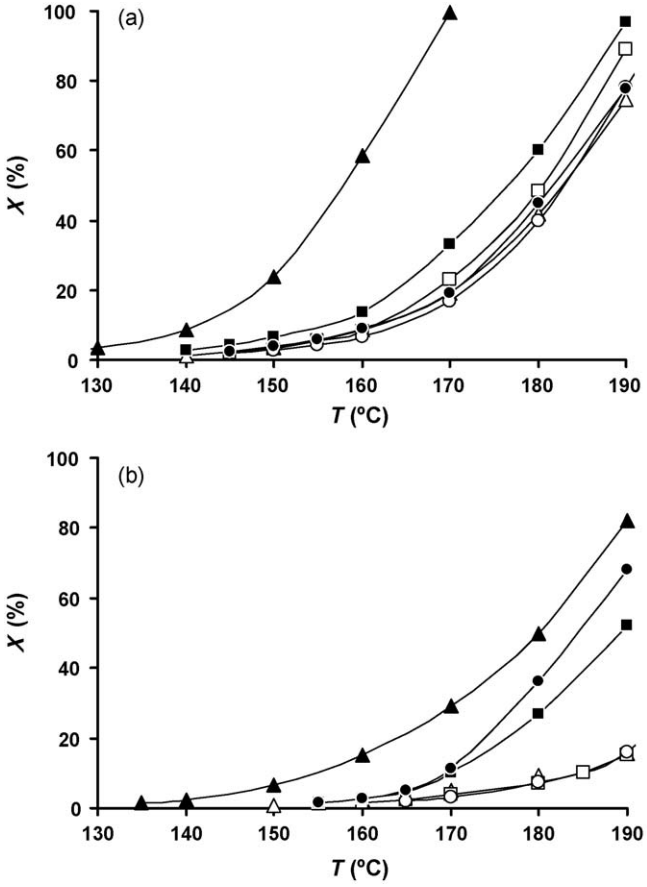

Fig. 7. Light-off curves for benzene (▲, △), toluene (■, □) and *m*-xylene (●, ○) combustion over (a) Pt catalysts and (b) Pd catalysts. Key: Closed symbols CNF-coated monolith catalysts; open symbols γ-Al_2O_3 coated monolith catalysts.

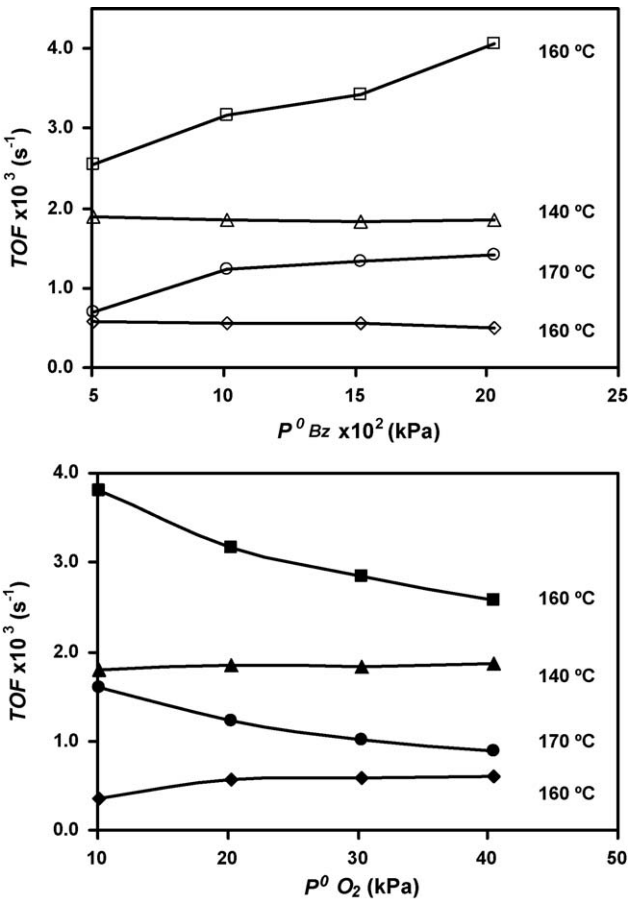

Fig. 8. Partial pressure effect of (a) benzene and (b) oxygen on the turn-over frequency of the catalysts in the benzene combustion. Key: Pt/ACNF (▲, △), Pd/ACNF (■, □), Pt/A (◆, ◇), Pd/A (●, ○).

Fig. 6 shows the light-off curves (the conversion as function of the reaction temperature) for benzene combustion; the conversions follow the sequence: Pt/ACNF > Pd/ACNF > Pt/A > Pd/A, that is, the monolith ACNF supported catalysts are the most active, in spite of the differences in metal loading and particle size among the catalysts; in fact catalysts supported on ACNF have the lowest metal loading (Table 4). The case of catalyst Pt/ACNF is rather interesting; it is a very active catalyst, especially for benzene combustion, showing activity even at 120 °C and reaching the complete benzene oxidation only at 170 °C at the applied space velocity. Furthermore, catalyst Pd/ACNF was more active than expected, even more than the catalyst Pt/A, which not only has a higher metal loading but also the metal particle size is considerably lower. Fig. 7 shows all the light-off curves for BTX combustion. Also here for each element, Pt (Fig. 7a) or Pd (Fig. 7b), those supported on monoliths ACNF always are the most active ones for the combustion of each aromatic compound. Catalysts supported on monoliths A seem to burn the three aromatic compounds with similar performance, but the ACNF supported catalysts burn benzene clearly better than toluene or *m*-xylene. Along this line, catalyst Pt/ACNF conversions followed the sequence: $X_{\text{Benzene}} > X_{\text{Toluene}} > X_{m\text{-Xylene}}$, which corresponds with earlier results for Pt/activated carbon catalysts obtained by Wu et al. [2]. These authors also showed that the order of BTX activity followed the order of adsorption of BTX, indicating that the oxidation rate is correlated with the surface concentration BTX. The dipolar moments for benzene, toluene and *m*-xylene are 0, 0.36 and 0.35 D, respectively [36], so if it is assumed that a surface pre-concentration improves the VOC combustion rate, our catalytic results are those expected, since the best VOC-carbon surface interaction is with the least polar benzene. Similar support effects have been proposed for the hydrogenation of cinnamaldehyde over CNF-supported Pt catalysts [17]. Similarly, in the work of Burgos et al. [16] on the deep oxidation of VOC mixtures over Pt supported on alumina monoliths was concluded that VOC's preferential adsorption on the polar alumina surface could be related to the polarity of the VOC.

In order to compare correctly the catalytic activity for total oxidation of benzene, toluene and *m*-xylene among the four catalysts, the intrinsic activity (expressed as turnover frequency, TOF (s^{-1})) was determined under differential conditions (conversion to $CO_2 < 10\%$) [21], at 150 °C or 160 °C depending on the activity of each catalyst. The exposed Pt and Pd surface area determined by chemisorption was used for the TOF calculations (Table 5). The TOF's followed the activity sequence reported above: Pt/ACNF > Pd/ACNF > Pt/A > Pd/A. So catalysts supported on CNF-coated monoliths are the most active, independently of the metal

Table 5
TOF [$\times 10^3$] data (s^{-1}) for the catalysts in the benzene combustion at 150 °C, and for toluene and *m*-xylene at 160 °C.

Catalysts	Bz (150 °C)	Tol (160 °C)	*m*-X (160 °C)
Pt/ACNF	5.07*	2.79*	1.95
Pd/ACNF	1.38	0.62	0.56
Pt/A	0.24	0.55	0.46
Pd/A	0.16	0.40	0.23

* Data obtained at ~15% conversion.

Table 6
Apparent reaction orders for benzene combustion at the indicated temperatures.

Catalyst	α_{Bz}	β_{O_2}	T (°C)
Pt/ACNF	-0.02 ± 0.01	0.02 ± 0.01	140
Pd/ACNF	0.32 ± 0.04	-0.27 ± 0.01	160
Pt/A	-0.09 ± 0.04	0.40 ± 0.12	160
Pd/A	0.51 ± 0.12	-0.42 ± 0.02	170

Pt or Pd or of the type of the aromatic compound tested. Clearly the influence of the kind of support used on the catalytic activity in these oxidation reactions plays an important role.

Finally, the TOF data also show that Pt catalysts always were more active than the Pd based ones on the same type of monolithic support.

3.4. Kinetic parameters of VOC oxidation

In the catalytic oxidation reaction of VOC, the reaction rate based on the simplest kinetic model can be expressed as:

$$r_{CO_2} = k[\mathrm{VOC}]^{\alpha}[O_2]^{\beta} \quad (1)$$

In a practical application, the concentration of oxygen normally is very much higher than the concentration of VOC, and the oxygen partial pressure can be considered constant during the reaction, and the observed rate will depend mainly only on the VOC concentration. Nevertheless, using Eq. (1) the reaction orders with respect to the benzene and oxygen concentration, as well as the apparent activation energies for combustion of BTX, were determined for all the catalysts for a quick comparison of the kinetic behaviour of the different catalysts. Measurements were obtained at differential conditions (conversion below 10%). Determination of reaction orders with respect to benzene was performed at constant temperature, oxygen partial pressure of 20.2 kPa, and between 5.1×10^2 and 20.3×10^2 kPa of benzene partial pressure. The reaction orders with respect to oxygen were performed at the same constant temperature as their corresponding ones of benzene, benzene partial pressure of 10.1×10^2 kPa (1036 ppm) and oxygen partial pressure between 10.1 and 40.4 kPa. Different temperatures have been employed for each catalyst, due to differences in activity. The results (Fig. 8 and Table 6) show that Pt and Pd catalysts have a different kinetic behaviour. The reaction orders in benzene for Pt are very close to zero or slightly negative, whereas they are always positive for Pd catalysts with values in the 0.3–0.6 range. The reaction order in oxygen for Pt catalysts depends on the support, being practically zero for catalyst Pt/ACNF, and 0.4 for Pt/A. The orders in oxygen for Pd catalysts are clearly negative. This indicates that the Pd catalyzed combustion of benzene is also inhibited by oxygen in our experimental conditions. The reaction orders obtained for the catalysts supported on monoliths A are very similar to those obtained by Papaefthimiou et al. [21]. The effect of the support is also clear from the observation that both reaction orders for catalysts supported on ACNF monoliths were always closer to zero than the corresponding ones for catalysts supported on monoliths A.

The apparent activation energies of the BTX reactions determined from the TOF data are collected in Table 7. The lowest activation energies over ACNF supported catalysts were observed for benzene, which was the least difficult to oxidize molecule (Table 5). For monolith A supported catalysts the activation energies do not point to a clear selectivity for some of the tested VOC's, nor do the TOF data (Table 5).

Some authors explain that combustion of single aromatic hydrocarbons over Pt catalysts can be interpreted by Langmuir–Hinshelwood kinetic models, which assume that the organic and oxygen are absorbed on active sites and react as adsorbed species [8,20]. However, other authors propose Eley–Rideal kinetic models where only oxygen is adsorbed on the active site and the VOC burnt from the gas phase without adsorption [16,22]. Moreover, different results have been published regarding the VOC adsorption strength on Pt; weakly adsorbed benzene [8], rapid and strong benzene adsorption [20]. The results of this work for benzene combustion collected in Fig. 8 and Table 6 seem to fit better with theories which propose adsorption of both reactants before reaction. The zero or low reaction order in benzene and oxygen, respectively, for the Pt catalysts suggests adsorption on different type of active sites (non-competitive), while the strong inhibition by oxygen in the case of Pd catalysts, suggests competition of both reactants for the same type of active sites. The pronounced effect of the CNF support suggests an important role in the adsorption location, especially for the Pt catalyst, but more detailed kinetic studies are required to reveal this.

3.5. Effects of water on the catalytic combustion

A possible explanation of the good performance of ACNF supported catalysts could be deduced from the water desorption profiles obtained by TPD (Fig. 9). It was observed that support A, after calcination in air at 400 °C and exposition to ambient air at room temperature for a month, could reincorporate important amounts of water (as adsorbed molecular water or like hydroxyl groups by reaction with the alumina surface) previously removed during the calcination treatment. Considering that catalysts were pre-treated *in situ* in H_2 flow at 300 °C, for catalysts used in the BTX combustion reactions, water should not appear below 300 °C during the TPD experiment; however Fig. 9 shows that a large amount of water evolved. This evolved water must originate from water produced during the combustion. So, the alumina can retain important amounts of the water molecules formed during the reaction, which could result in a decrease on the catalytic activity due to competitive adsorption; it has been shown that surface hydroxyls are formed on Pd and Pd–Pt catalysts supported on Al_2O_3 during methane combustion at 200 °C [1]. Moreover, TPD-results agree with the obtained water immersion enthalpies (Table 2) which show that monolith ACNF is more hydrophobic than monolith A, and so, CNF-coated monoliths are superior support of Pt or Pd catalysts in the gas phase catalytic combustion of BTX.

Table 7
Apparent activation energies (kJ/mol) and pre-exponential factor (s^{-1}) obtained by Arrhenius equation from TOF data.

Catalyst	Benzene		Toluene		*m*-Xylene	
	E_A	A	E_A	A	E_A	A
Pt/ACNF	122 ± 2	5.0×10^{12}	128 ± 1	8.5×10^{12}	131 ± 3	1.1×10^{13}
Pd/ACNF	145 ± 1	1.1×10^{15}	161 ± 3	1.7×10^{16}	165 ± 1	4.6×10^{16}
Pt/A	138 ± 4	2.5×10^{13}	138 ± 5	2.8×10^{13}	138 ± 3	1.9×10^{13}
Pd/A	122 ± 6	2.5×10^{11}	116 ± 4	5.0×10^{10}	142 ± 2	5.1×10^{13}

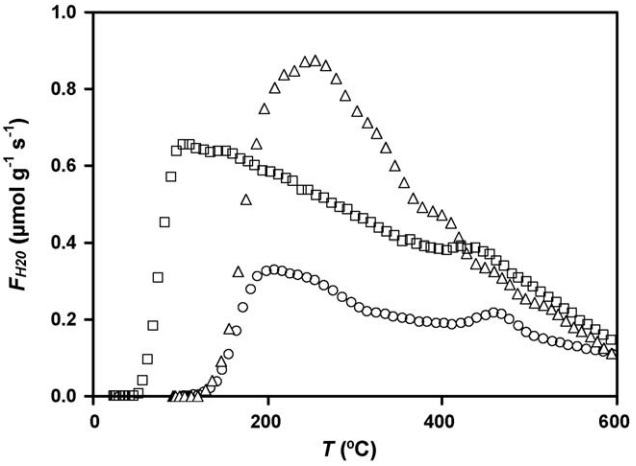

Fig. 9. Water desorption profiles obtained by TPD. Key: Freshly prepared support A (△); Support A calcined at 400 °C and exposed to ambient air at room temperature (○); Catalyst Pt/A after reaction (□).

Table 8
Decrease in conversion (%), relative to the original conversion, for benzene combustion in presence of water steam (22,000 ppm) in the reactant flow at different reaction temperatures.

T (°C)	Pt/ACNF	Pt/A	Pd/ACNF	Pd/A
160	7.7	24.4	81.1	83.4
170	7.6	24.6	83.4	82.1
180	–	24.4	80.2	85.5

It is known that moisture influences VOC oxidation in most situations, especially at low temperatures. As a general rule, water has been found to act as inhibitor of VOC oxidation over Pt and Pd catalyst supported on inorganic oxides [1,3]. For this reason, the effect of water on the intrinsic activity of the catalysts has been studied in the benzene combustion, as an example. Taking in account that in the case of input streams from air stripping of VOC's contained in contaminated water, the water content can exceed 10,000 ppm, the performance of the catalysts was examined employing a feed mixture containing 1036 ppm of benzene and 22,000 ppm of water vapour. The reduction in conversion to CO_2 at different reaction temperatures is presented in Table 8. In all the cases the original conversions were recovered when water was removed from the feed to their original values. Pt catalysts are much less affected by the presence of water than Pd catalysts. In fact the catalytic activity of Pd catalysts practically disappears when water is present in the feed. This phenomenon also suggests that water competes strongly with oxygen for the Pd active sites, next to its strong adsorption on the support. This could explain why Pt is more active than Pd when deposited on the same kind of monolithic support (Table 5). Water produced during reaction cannot only be retained on the catalyst support but also inhibits the Pd catalyzed reaction. This double water effect is observed in Table 8 as well, where the decrease in conversion for Pt catalysts in the presence of water vapour was very different depending on the support (both catalysts have very similar particle size). While the activity of Pt/ACNF decreased less than 8%, the activity of Pt/A decreased around the 25%. Finally, Pd catalysts on both supports suffered equally and strongly from the presence of water in the feed, suggesting that the competitive adsorption on the Pd dominates that on the support, if the latter has any effect at all.

4. Conclusions

Carbon nanofiber (CNF)-coated monoliths with a very thin, homogeneous, consistent and good adhered CNF layer were obtained by means of catalytic decomposition of ethylene on Ni particles.

The catalysts supported on CNF-coated monoliths showed a preference to burn benzene better than toluene or *m*-xylene, which is ascribed to a better aromatic-support dispersive interaction. Pt/ACNF showed always the best performance, and was already active at 120 °C in the benzene combustion reaching full conversion at 170 °C. In all cases CO_2 and H_2O were always the only reaction products found.

CNF-coated monoliths are superior supports over alumina for Pt or Pd catalysts in the gas phase catalytic combustion of BTX at low temperatures. The CNF-coated monolith catalysts were the most active, independently of the metal or the type of the tested aromatic compound. This seems to be due to the fact that the CNF surface is more hydrophobic than that of γ-Al_2O_3, and the release of water molecules produced during the combustion is favoured.

Pt catalysts showed apparent reaction orders in benzene around zero whereas the corresponding reaction orders for Pd catalysts always were positive with values in the 0.3–0.6 range. Apparent reaction orders in oxygen for Pt catalysts were found positive and very close to zero, whereas the corresponding ones for Pd catalysts were clearly negative, indicating that the Pd catalyzed combustion of benzene is inhibited by oxygen. Water also is a strong inhibitor of the Pd catalyzed combustion of benzene.

BTX combustion is catalyzed by Pt and Pd through different kinetic mechanisms, and accounts for the fact that Pt catalysts were always more active than the Pd ones on the same type of support.

Acknowledgements

A.F. Pérez-Cadenas and S. Morales-Torres acknowledge the Spanish Ministry of Education and Science for a Ramón y Cajal research contract and for a F.P.U research fellowship, respectively. The authors acknowledge Corning Inc. for supplying the monoliths. These investigations were supported by the MEC-FEDER and the Junta de Andalucía, projects CTQ2006-04702, CTQ2007-61324 and RNM 547.

References

[1] K. Persson, L.D. Pfefferle, W. Schwartz, A. Ersson, S.G. Jaras, Appl. Catal. B: Environ. 74 (2007) 242–250.
[2] J.C.-S. Wu, Z.A. Lin, F.M. Tsai, J.W. Pan, Catal. Today 63 (2000) 419–426.
[3] P. Papaefthimiou, T. Ioannides, X.E. Verykios, Appl. Catal. B: Environ. 15 (1998) 75–92.
[4] A. Quintanilla, J.J.W. Bakker, M.T. Kreutzer, J.A. Moulijn, F. Kapteijn, J. Catal. 257 (2008) 55–63.
[5] M. Zhang, B. Zhou, K.T. Chuang, Appl. Catal. B: Environ. 13 (1997) 123–130.
[6] F.J. Maldonado-Hódar, C. Moreno-Castilla, A.F. Pérez-Cadenas, Appl. Catal. B: Environ. 54 (2004) 217–224.
[7] M.A. Alvarez-Merino, M.F. Ribeiro, J.M. Silva, F. Carrasco-Marin, F.J. Maldonado-Hodar, Environ. Sci. Technol. 38 (2004) 4664–4670.
[8] I. Mazzarino, A.A. Barresi, Catal. Today 17 (1993) 335–347.
[9] P. Bardhan, Curr. Opin. Solid State Mater. Sci. 2 (1997) 577–583.
[10] T. Boger, M.M.P. Zieverink, M.T. Kreutzer, F. Kapteijn, J.A. Moulijn, W.P. Addiego, Ind. Eng. Chem. Res. 43 (2004) 2337–2344.
[11] F. Kapteijn, R.M. de Deugd, J.A. Moulijn, Catal. Today 105 (2005) 350–356.
[12] X. Xu, H. Vonk, A.C.J.M. van de Riet, A. Cybulski, A. Stankiewicz, J.A. Moulijn, Catal. Today 30 (1996) 91–97.
[13] F. Kapteijn, J.J. Heiszwolf, T.A. Nijhuis, J.A. Moulijn, Cattech 3 (1999) 24–41.
[14] A.F. Pérez-Cadenas, F. Kapteijn, J.A. Moulijn, F.J. Maldonado-Hódar, F. Carrasco-Marín, C. Moreno-Castilla, Carbon 44 (2006) 2463–2468.
[15] A.F. Perez-Cadenas, S. Morales-Torres, F. Kapteijn, F.J. Maldonado-Hodar, F. Carrasco-Marin, C. Moreno-Castilla, J.A. Moulijn, Appl. Catal. B: Environ. 77 (2008) 272–277.
[16] N. Burgos, M. Paulis, M. Mirari Antxustegi, M. Montes, Appl. Catal. B: Environ. 38 (2002) 251–258.
[17] M.L. Toebes, T.A. Nijhuis, J. Hajek, J.H. Bitter, A. Jos van Dillen, D.Y. Murzin, K.P. de Jong, Chem. Eng. Sci. 60 (2005) 5682–5695.
[18] V. de Jong, M.K. Cieplik, W.A. Reints, F. Fernandez-Reino, R. Louw, J. Catal. 211 (2002) 355–365.
[19] S. Ordonez, L. Bello, H. Sastre, R. Rosal, F.V. Diez, Appl. Catal. B: Environ. 38 (2002) 139–149.

[20] T.F. Garetto, C.R. Apesteguia, Appl. Catal. B: Environ. 32 (2001) 83–94.
[21] P. Papaefthimiou, T. Ioannides, X.E. Verykios, Appl. Catal. B: Environ. 13 (1997) 175–184.
[22] S.K. Gangwal, M.E. Mullins, J.J. Spivey, P.R. Caffrey, B.A. Tichenor, Appl. Catal. 36 (1988) 231–247.
[23] A.A. Barresi, M. Cittadini, Int. J. Environ. Studies 57 (2000) 179–188.
[24] K.P. de Jong, J.W. Geus, Catal. Rev. -Sci. Eng. 42 (2000) 481–510.
[25] A.F. Perez-Cadenas, F. Kapteijn, J.A. Moulijn, Appl. Catal. A: Gen. 319 (2007) 267–271.
[26] T.A. Nijhuis, A.E.W. Beers, T. Vergunst, I. Hoek, F. Kapteijn, J.A. Moulijn, Catal. Rev. -Sci. Eng. 43 (2001) 345–380.
[27] C. Prado-Burguete, A. Linares-Solano, F. Rodriguez-Reinoso, C.S.-M. de Lecea, J. Catal. 115 (1989) 98–106.
[28] A.F. Pérez-Cadenas, M.M.P. Zieverink, F. Kapteijn, J.A. Moulijn, Catal. Today 105 (2005) 623–628.
[29] S. Brunauer, P.H. Emmet, E. Teller, J. Am. Chem. Soc. 60 (1938) 309–319.
[30] R.C. Bansal, J.B. Donnet, F. Stoeckli, Active Carbon, M. Dekker, New York, 1988 (Chapter 4, pages 164–183).
[31] M.A. Alvarez-Merino, F. Carrasco-Marín, J.L.G. Fierro, C. Moreno-Castilla, J. Catal. 192 (2000) 363–373.
[32] M. Gurrath, T. Kuretzky, H.P. Boehm, L.B. Okhlopkova, A.S. Lisitsyn, V.A. Likholobov, Carbon 38 (2000) 1241–1255.
[33] A.L. Dantas Ramos, P.D.S. Alves, D.A.G. Aranda, M. Schmal, Appl. Catal. A: Gen. 277 (2004) 71–81.
[34] C.D. Wagner, W.M. Riggs, L.E. Davis, J.F. Moulder, G.E. Muilenberg (Eds.), Handbook of X-Ray Photoelectron Spectroscopy, Perkin-Elmer, Physical Electronics Division, Eden Prairie, MI, 1978.
[35] M.T. Kreutzer, J.J.W. Bakker, F. Kapteijn, J.A. Moulijn, P.J.T. Verheijen, Ind. Eng. Chem. Res. 44 (2005) 4898–4913.
[36] R.C. Weast (Ed.), CRC Handbook of Chemistry and Physics, CRC Press, Florida, 1980